ISSN 1392–1320 MATERIALS SCIENCE (MEDŽIAGOTYRA). Vol. XX, No. X. 2022

Water Safety for Human Health: Detection of Pollutants by Blue-Emission Carbon Quantum Dots via Three Modes in Different Polluted Water Bodies

Shujuan DAI [1], Xiaoliang HAO [2] *, Zhigang FANG [2], Jing GUO [3], Yingxue TENG [3]

[1] *College of Mining Engineering, University of Science and Technology Liaoning, Anshan 114051, PR China*
[2] *College of Chemical Engineering, University of Science and Technology Liaoning, Anshan 114051, PR China*
[3] *College of Materials and Metallurgy, University of Science and Technology Liaoning, Anshan 114051, PR China*

crossref http://dx.doi.org/10.5755/j02.ms.25054

Received 10 January 2020; accepted 06 August 2020

Water quality directly affects human health. It is very important to design a probe that can detect the pollutants in water. In this study, we synthesized one kind of carbon dots (CDs), which could emit strong blue fluorescence. The blue fluorescence could be quenched by 2,4,6-trinitrophenol (TNP) ascribed to the energy transfer (ET), could be quenched by lemon yellow (LY) ascribed to inner filter effect (IFE), and could be quenched by HClO ascribed to surface passivation (SP). TNP, LY, and HClO are common contaminants in water. By our experiment, it was proved that the synthesized CDs are a safe and effective fluorescent material and could be used to detect the pollutants (TNP, LY, and HClO) in the actual water sample.
Keywords: carbon dots, fluorescent probes, lemon yellow, pollution.

1. INTRODUCTION

Development of industry has led to overuse of many pollutants such as fertilizers, herbicides, and pesticides, which easily get into the water system, sometimes even get directly discharged into surface water [1]. Pollutants in water have a direct threat to the safety of public health [2]. Moreover, the food additives are widely used in the food industry, such as pigments and flavors, which cause a serious threat to people's health [3]. Human activities such as dye industry, washing, also contribute different pollutants to waters [4].

The carbon dots (CDs) are excellent nanomaterials, and could be used for detecting various pollutants. Most of these studies were based on detecting of only one or two pollutants [5]. Realizing that multimode sensing is the better option than detecting one pollutant, some researchers have made significant progress in this direction.

A variety of pollutants synthesized by human beings bring a certain threat to the safety of water bodies. Among these pollutants, 2,4,6-trinitrophenol (TNP), lemon yellow (LY), and hypochlorous acid (HClO) are three representative types. TNP has been most widely used in fuel industry, chemical products and other industries [6]. LY is one of many food additives, which has been widely used in the beverage industry, fruit and wine products [7]. HClO is an important disinfectant and often used for the disinfection of ponds, rivers, swimming pools [8]. The three substances are common water pollutants, and the detections for them are crucial for public health.

In this work, we synthesized one certain kind of CDs which could be used to detect three kinds of pollutants in the water, TNP, LY, and HClO. Although three substances are widely found in water bodies, TNP is mainly used in the heavy industry, LY is often used in the food industry, and HClO is mainly used in the purification of water body.

By the blue fluorescence, we could detect TNP, LY and HClO in some water samples (TNP: waste water and washing water, LY: soft drink and cocktail, and HClO: lake water and tap water). The detection mechanisms for TNP, LY and HClO are energy transfer (ET), inner filter effect (IFE), and surface passivation (SP), respectively (Fig. 1). There are many active sites in the TNP structure, which easily lead to electron transfer. These electrons are transferred between TNP and CDs, causing the fluorescence disappear. LY has ultraviolet absorption, which can shield the fluorescence by overlapping the signals between ultraviolet and fluorescence. There are many oxygen free radicals on HClO. These free radicals are highly oxidative and can passivate the surface of CDs.

2. EXPERIMENTAL PROCEDURES

The following analytical techniques were employed: transmission electron microscopy (TEM, Hitachi H-7700); UV-vis absorption spectra (UV-2000 UV-vis spectrophotometer, Unico China); fluorescence detection (FL-2700 fluorescence spectrometer, Hitachi Japan); X-ray diffraction (XRD) (Bruker AXS, Germany); Fourier transform infrared spectrometer (FTIR) (Mettle, Switzerland); X-ray photoelectron spectroscopy (XPS) (ESCALAB250Xi, Thermo Scientific); fluorescence life time (FLS 920 fluorescence spectrophotometer, Edinburgh Instruments Ltd).

0.2 g malic acid was measured accurately and dissolved with 20 mL ethanolamine, made to undergo ultrasound for 10 minutes, placed into Teflon autoclave, and heating for 4 h at 180 °C. Organic solvents were removed by vacuum distillation and dried in a 60 °C vacuum drying chamber. The dispersion of the synthesized CDs is very good, and they can be miscible with water in any proportion.

* Corresponding author. Tel.: +86-4125929271; fax: +86-4125929272.
E-mail address: *haoxiaoliang1980@163.com* (X. Hao)

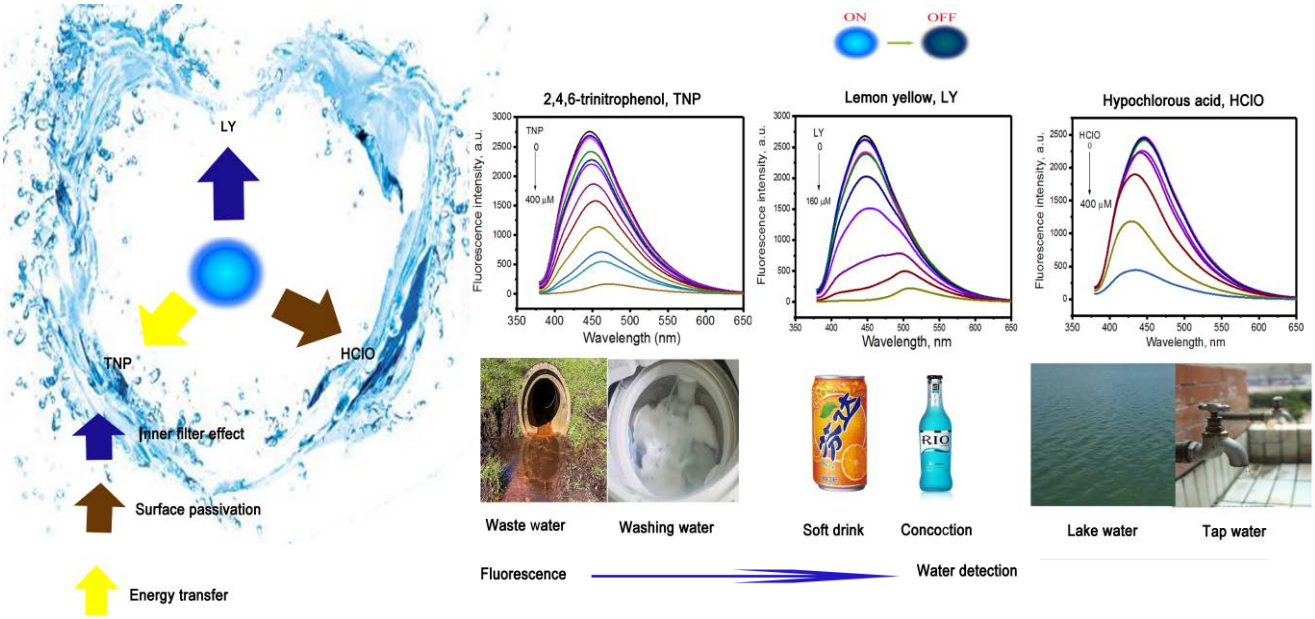

Fig. 1. The detection mechanisms for TNP, LY and HClO (energy transfer, inner filter effect and surface passivation)

Phosphoric acid buffer (PBS) was used for all the detection work. In order to evaluate whether this method could be used to detect TNP, LY and HClO, the recovery experiments were pursued. The detection systems of TNP, LY and HClO were that: industry wastewater and washing water, fanta soft drink and RIO cocktail, tap water and lake water, respectively. The wastewater was sampled from the factory pipe, the washing water was obtained from an automatic washing machine in the dormitory building, fanta soft drink and RIO cocktail were from the local supermarket, and the lake water and tap water were from the surrounding areas. Fanta soft drink and RIO cocktail were diluted to 100 times.

3. RESULTS

A quantum yield of 18.98 % was achieved using quinine sulfate method [5]. The microstructure of the CDs was analysed by TEM. Their shape was approximately spherical and the size was uniform, the average diameter was measured as 5.67 ± 0.26 nm (see Fig. 2 a, Fig. 2 b).

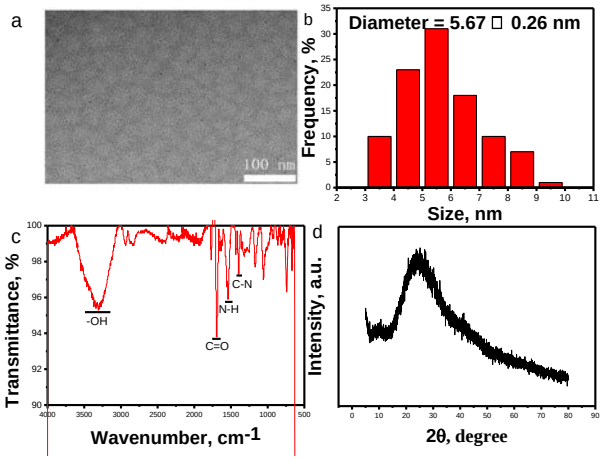

Fig. 2. a – TEM image; b – average diameter, c – FTIR spectrum; d – X-ray diffraction pattern

The surface groups were analysed by FTIR (Fig. 2 c). The band at 3306 cm^{-1} was –OH. 1402 cm^{-1} was C–N. 1688 and 1553 cm^{-1} were ascribed to C=O and N–H [9, 10].

Crystalline was analysed by X-ray diffraction (Fig. 2 d). A diffraction peak (2θ) at 23.75 was observed, it indicating the crystalline structure of the CDs is presumed to be similar to the (002) lattice spacing of graphitic-like carbon based materials [11].

Three dominant peaks (C1s, N1s, and O1s) are at 285, 400 and 532 eV in the XPS (Fig. 3 a). The high-resolution spectrum depicts C1s has C–C/C=C states (Fig. 3 b). The high-resolution N1s XPS spectrum exhibits one peak of at 400 eV, representing N1s states in pyrrolic-like N (Fig. 3 c). The O1s spectrum 532 eV (Fig. 3 d), proving the C–OH/C–O–C groups, respectively [12].

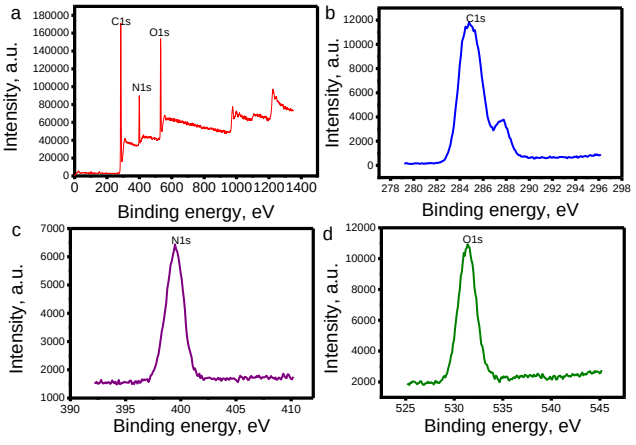

Fig. 3. a – XPS spectrum. The high resolution XPS spectra: b – C1s; c – N1s; d – O1s

Time-resolved fluorescence spectra of the CDs were collected for 446 nm at an excitation wavelength fixed at 360 nm (Fig. 4). From the decay curve, the average lifetime $\tau_{average}$ is equal to 0.40 ns. The lifetime shows the basic characteristics of typical fluorescent materials.

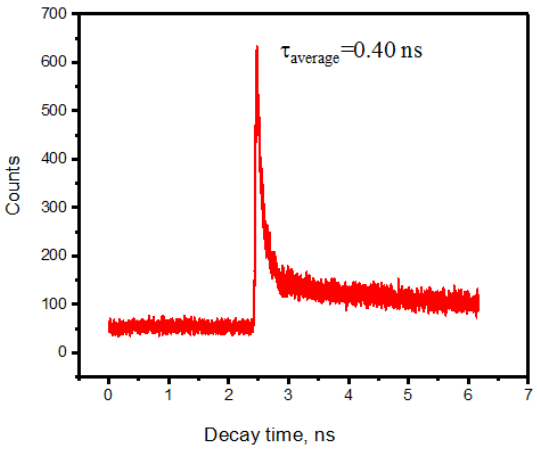

Fig. 4. The fluorescence lifetime of the CDs

UV-vis spectrum is depicted in Fig. 5 a (1). The peak of 250 nm might ascribe to the $\pi \rightarrow \pi^*$ transition. The peak of 300 – 500 nm might be the $n \rightarrow \pi^*$ transition [13, 14]. The excitation (Fig. 5 a (2)) and emission spectra (Fig. 5 a (3)) were also acquired in Fig. 5 a.

The fluorescence intensities under different excitation are compared (Fig. 5 b). As excitation wavelength increased, fluorescence intensities were decreased, indicating that the CDs exhibited excitation dependence.

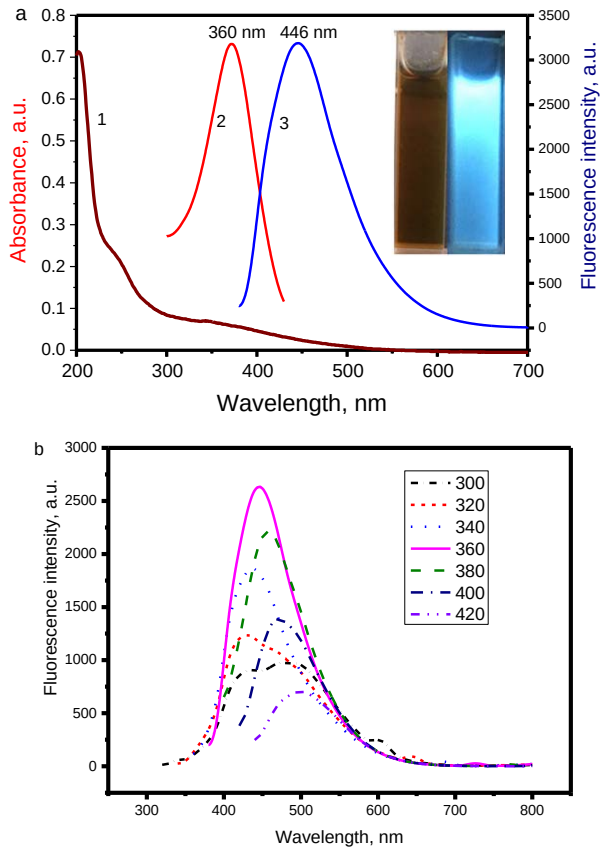

Fig. 5. a – 1 UV-Vis, 2 excitation, 3 emission. Inset: CDs water solution and its fluorescence; b – fluorescence at different wavelengths

The photostability of the CDs was compared. By experiment, it was seen that the CDs were stabilized within 60 min (Fig. 6 a). The influence of ionic strength was also researched (Fig. 6 b), it can be seen that the CDs are relatively stable for ionic strength. The fluorescence intensities remained unchanged, indicating that the CDs had acid-base stability (Fig. 6 c). pH 7.0 is the neutral condition, the damage of inner structure for materials by strong acid and strong base was avoided, suitable for analysis of real samples.

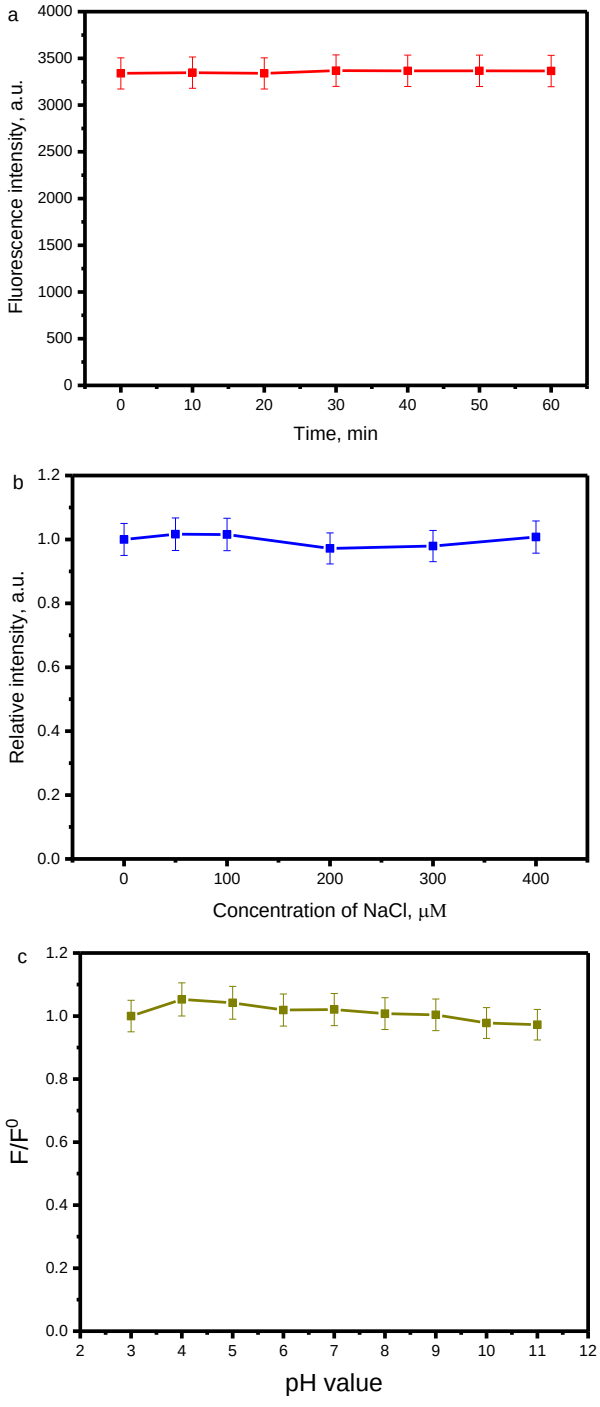

Fig. 6. a – photostability of the CDs; b – influence of ionic strength; c – influence of pH

Interferences of external conditions to CDs were also studied. In the experiments, we used some conventional metal ions (Fig. 7 a), anions (Fig. 7 b), and other aditives (Fig. 7 c), including Galactose, Fructose, Uric acid, VC, Valine, Thiourea, Dopamine, Maltose, Lysine, Histidine, Phenylalanine, Malic acid, Threonine, Alanine, Serine, Imidazole, Leucine, Tyrosine, Glutamate, Glutathione,

Glucose, Glycine, Aspartic acid, Proline, Xylose, Cysteine. It could be seen that no matter metal ions, anions, or other interferences, had few influence on the CDs.

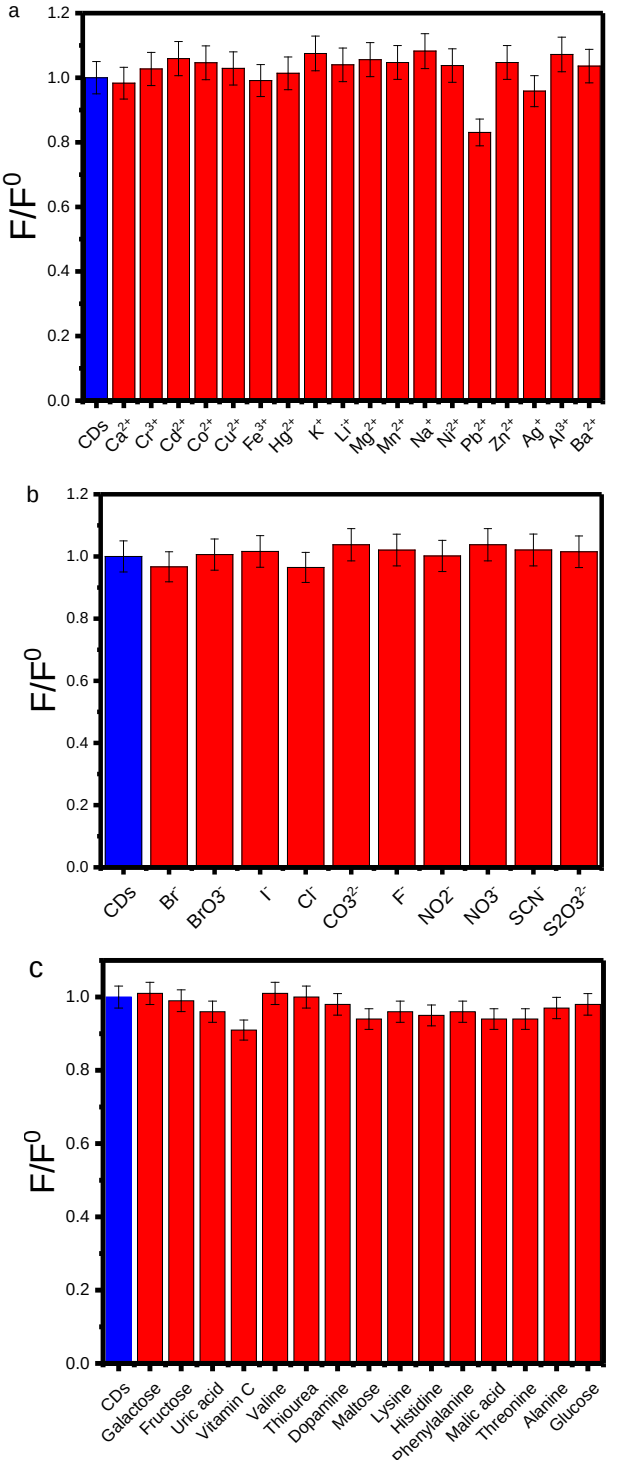

Fig. 7. Interferences: a – metal ions; b – anions; c – other reagents

4. DESIGN OF THE CDS PROBE TO DETECT TNP, LY, AND HClO

Fig. 8 a depicts that TNP had no fluorescence. The inset depicted the energy was transferred between TNP and CDs. The reaction time which TNP quenched the fluorescence of the CDs was very short (Fig. 8 b). The quenching mechanism was inferred that there were three phenolic hydroxyl groups in TNP, the phenolic hydroxyl groups have strong activity, when TNP was added into the CDs solution, the energy was transferred between TNP and CDs, the loss of energy caused the disappearance of fluorescence.

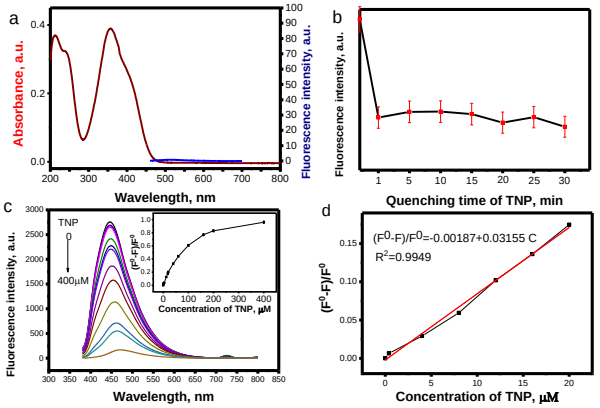

Fig. 8. a – UV-vis and the fluorescence spectra of TNP. Inset: the mechanism of energy transfer between TNP and CDs; b – the quenching time of TNP; c – quenching of fluorescence intensity by TNP. Inset: quenching rate with the addition of TNP; d – linear relationship between quenching rate and TNP

When TNP was added, the fluorescence intensity decreased gradually (Fig. 8 c). A linear equation was obtained (Fig. 8 d), where F^0 is defined as the fluorescence intensity in the initial state, F is defined as the fluorescence intensity at different LY concentrations, and C is the concentration of LY, respectively. Limited of detection (LOD) for TNP was 0.51 μM. A IFE occurred between the LY and CDs (Fig. 9 a). It was concluded that LY had no fluorescence, proving that the fluorescence quenching was due to IFE. Fig. 9 b depicted the quenching time of LY, it was seen that quenching reaction needed a shorter time.

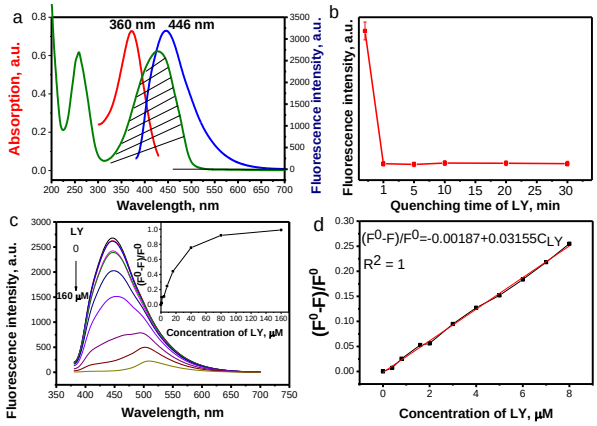

Fig. 9. a – UV-vis, the fluorescence of LY, excitation, and emission spectra of CDs; b – the quenching time of LY; c – quenching of fluorescence intensity by LY. Inset: quenching rate with the addition of LY; d – linear relationship between quenching rate and LY

HClO had the oxidability, following the reaction: $HClO = H^+ + Cl^- + O$, oxygen radicals (O) could passivate the surface groups of CDs and cause fluorescence quenching. Fig. 10 a indicates that HClO had no fluorescence, the central peak of HClO is 300 nm, which proved that there was no IFE. The surface groups were

passivated by oxygen radicals decomposed by HClO, so the fluorescence was quenched [15, 16]. The quenching time of HClO was also investigated, we could conclude from Fig. 10 b that the quenching reaction would occur in a shorter time. Similar quenching phenomenon occurred between the CDs and HClO (Fig. 10 c). A linear equation was acquired (Fig. 10 d). The LOD for HClO was estimated to be 0.98 μM.

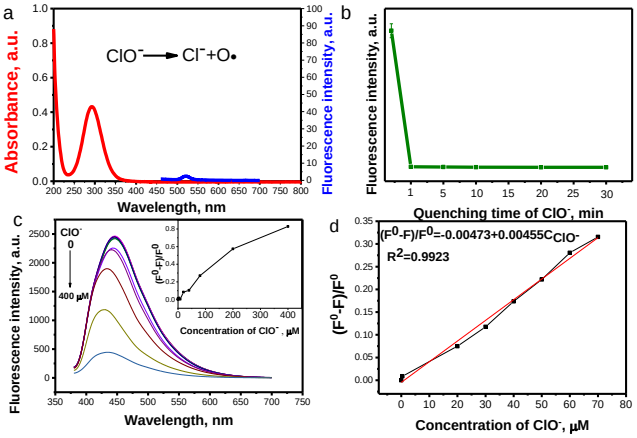

Fig. 10. a – UV-vis and fluorescence spectra of ClO^-; b – the quenching time of ClO^-; c – quenching of fluorescence intensity by ClO^-. Inset: quenching rate with the addition of ClO^-; d – linear relationship between quenching rate and ClO^-

We could detect LY via IFE (Fig. 9 c). When the quantity of LY was added, the fluorescence was gradually quenched. A linear equation was acquired (Fig. 9 d). The LOD for LY was 0.14 μM.

As presented in Table 1, Table 2 and Table 3, the recoveries of TNP, LY, and ClO^- were detected. These pollutants have been effectively recovered in different water bodies and the deviations are within the acceptable range.

Table 1. Analytical results for the detection of TNP in waste water and washing water

Sample	Concentration of TNP, μM	Total found, μM	Recovery (%), N=3	RSD[a] (%), N=3
Waste water	9.0	9.0	100.5	5.9
	18.0	18.9	104.8	3.9
	20.0	21.5	107.7	2.8
Washing water	9.0	9.4	104.1	6.8
	18.0	18.7	104.0	3.4
	20.0	20.6	103.2	2.6

[a] Relative standard deviation (RSD) was defined as (standard deviation/mean) × 100 %

Table 2. Analytical results for the detection of lemon yellow in soft drink and cocktail

Sample	Concentration of ClO^-, μM	Total found, μM	Recovery (%), N=3	RSD (%), N=3
Tap water	24.0	24.2	100.8	5.4
	38.0	37.7	99.3	1.7
	64.0	62.1	97.0	1.0
Lake water	24.0	24.6	102.7	1.0
	38.0	38.5	101.4	1.8
	64.0	63.8	99.7	0

Table 3. Analytical results for the detection of ClO^- in tap water and lake water

Sample	Concentration of LY, μM	Total found, μM	Recovery (%), N=3	RSD (%), N=3
Fanta soft drink	2.2	2.4	108.0	6.2
	5.0	5.1	102.2	3.0
	7.0	7.3	104.0	1.5
RIO cocktail	2.2	2.2	99.9	3.4
	5.0	4.8	96.1	0.6
	7.0	7.1	102.0	2.1

5. DISCUSSION AND CONCLUSIONS

Multimodal detection has been the one of research directions for many researchers. At first, people can only detect one substance by one mode, for example, metronidazole is detected by ET [17]. Later improvements were made, three kinds of metal ions are detected by changing the buffer solution [16], three kinds of medicines were analysed by switching different quenching manners [5] and triple-mode emissions were also studied [18].

Compared with some reports above, in this work, we designed three different modes (ET, IFE and SP). Firstly, the detection mechanisms are different from the existing literature.

Secondly, the three detection modes which we used are different in mechanism themselves (Fig. 1). Compared with other analysis, due to different quenching mechanism, the interferences among detection substances are relatively small.

Thirdly, the object of our study is the detection of pollutants in the water. Compared with other pollutants in the natural environment, the pollutants in the water are relatively smaller, this is one of the prerequisites for our successful detection. In addition, in the three detection modes, the detection efficiencies of ET and SP are higher than IFE, because the IFE detection is more susceptible to the interference of other pollutants. In our study, the test objects we used were softdrinks and cocktails, because the other additives in these two foods are relatively less, so we have achieved relatively good detection results.

Finally, compared with chemical methods and other instrument analysis methods, the fluorescence detection method is simpler. We can even use the hand-held ultraviolet lamp of the money detector to detect the fluorescence. Meanwhile, the fluorescent material in this study is synthesized by carbonizing at high temperature, therefore have higher safety. Of course, there are still some deficiencies in our study, such as the detection of heavy pollutants is still difficult to achieve. In addition, the multi-mode used in this study is for different water bodies, we preliminarily divided the water into three categories: ET mechanism for industrial water detection, IFE mechanism for beverage water detection, and SP mechanism for living water detection, so there is a premise for detection. In the future, we hope that by our efforts, this material can be developed into a kit to detect pollutants in different water bodies and contribute to environmental protection and people's health.

Acknowledgments

We are very grateful to National Natural Science Foundation of China (project number: U1860112) for its help.

REFERENCES

1. **Bettez, N.D., Marino, R., Howarth, R.W., Davidson, E.A.** Roads as Nitrogen Deposition Hot Spots *Biogeochemistry* 114 (1 – 3) 2013: pp. 149 – 163. https://doi:10.1007/s10533-013-9847-z
2. **Ma, J., Reckhow, D., Xie, Y.Y.** Drinking Water Safety: Science, Technology, Engineering and Policy *Frontiers of Environmental Science & Engineering* 9 2015: pp. 2. https://doi:10.1007/s11783-015-0771-4
3. **Shah, R., Kolanos, R., DiNovi, M.J., Mattia, A., Kaneko, K.J.** Dietary Exposures for the Safety Assessment of Seven Emulsifiers Commonly Added to Foods in the United States and Implications for Safety *Food Additives & Contaminants: Part A* 34 (6) 2017: pp. 905 – 917. https://doi.org/10.1080/19440049.2017.1311420
4. **Karfa, P., Roy, E., Patra, S., Kumar, S., Tarafdar, A., Madhuri, R., Sharma, P.K.** Amino Acid Derived Highly Luminescent, Heteroatom-doped Carbon Dots for Label-free Detection of Cd^{2+}/Fe^{3+}, Cell Imaging and Enhanced Antibacterial Activity *RSC Advances* 5 2015: pp. 58141 – 58153. https://doi: 10.1039/c5ra09525e
5. **Li, C., Liu, W.J., Sun, X.B., Pan, W., Yu, G.F., Wang, J.P.** Excitation Dependent Emission Combined with Different Quenching Manners Supports Carbon Dots to Achieve Multi-mode Sensing *Sensors and Actuators B* 263 2018: pp. 1 – 9. https://doi:10.1016/j.snb.2018.02.050
6. **Shi, D.C., Yan, F.Y., Zheng, T.C., Wang, Y.Y., Zhou, X.G., Chen, L.** P-doped Carbon Dots Act as a Nanosensor for Trace 2, 4, 6-trinitrophenol Detection and a Fluorescent Reagent for Biological Imaging *RSC Advances* 5 2015: pp. 98492. https://doi:10.1039/c5ra18800h
7. **Xu, H., Yang, X.P., Li, G., Zhao, C., Liao, X.J.** Green Synthesis of Fluorescent Carbon Dots for Selective Detection of Tartrazine in Food Samples *Journal of Agricultural and Food Chemistry* 63 2015: pp. 6707 – 6714. https://doi:10.1021/acs.jafc.5b02319
8. **Zhang, Z.W., Pei, K., Yang, Q.L., Dong, J.Y., Yan, Z.Y., Chen, J.Q.** Nanosensor of Sulfur-nitrogen Co-doped Carbon Dots for "off-on" Sensing of Hypochlorous Acid and Zn(II) and Its Bioimaging *New Journal of Chemistry* 42 (19) 2018: pp. 15895 – 15904. https://doi:10.1039/c8nj03159b
9. **Vikneswaran, R., Ramesh, S., Yahya, R.** Green Synthesized Carbon Nanodots as a Fluorescent Probe for Selective and Sensitive Detection of Iron(III) Ions *Materials Letters* 136 2014: pp. 179 – 182. https://doi:10.1016/j.matlet.2014.08.063
10. **Lan, M.H., Di, Y.F., Zhu, X.Y., Ng, T.W., Xia, J., Liu, W.M., Meng, X.M., Wang, P.F., Lee, C.S., Zhang, W.J.** A Carbon Dot-based Fluorescence Turn-on Sensor for Hydrogen Peroxide with a Photo-induced Electron Transfer Mechanism *Chemical Communications* 51 2015: pp. 15574 – 15577. https://doi:10.1039/c5cc05835j
11. **Du, F.F., Gong, X.J., Lu, W.J., Liu, Y., Gao, Y.F., Shuang, S.M., Xian, M., Dong, C.** Bright-green-emissive Nitrogen-doped Carbon Dots as a Nanoprobe for Bifunctional Sensing, Its Logic Gate Operation and Cellular Imaging *Talanta* 179 2018: pp. 554 – 562. http://doi:10.1016/j.talanta.2017.11.030
12. **Pattison, D.I., Davies, M.J., Hawkins, C.L.** Reactions and Reactivity of Myeloperoxidase-derived Oxidants: Differential Biological Effects of Hypochlorous and Hypothiocyanous Acids free *Radical Research* 46 (8) 2012: pp. 975 – 995. https://doi:10.3109/10715762.2012.667566
13. **Ganiga, M., Cyriac, J.** Understanding the Photoluminescence Mechanism of Nitrogen-doped Carbon Dots by Selective Interaction with Copper Ions. *Chemphyschem* 17 2016: pp. 2315 – 2321. https://doi:10.1002/cphc.201600294
14. **Dong, X.W., Wei, L.M., Su, Y.J., Li, Z.L., Geng, H.J., Yang, C., Zhang, Y.F.** Efficient Long Lifetime Room Temperature Phosphorescence of Carbon Dots in a Potash Alum Matrix *Journal of Materials Chemistry C* 3 2015: pp. 2798 – 2801. https://doi:10.1039/c5tc00126a
15. **Liu, M., Xu, Y., Niu, F., Gooding, J.J., Liu, J.** Carbon Quantum Dots Directly Generated from Electrochemical Oxidation of Graphite Electrodes in Alkaline Alcohols and the Applications for Specific Ferric Ion Detection and Cell Imaging *Analyst* 141 2016: pp. 2657 – 2664. https://doi:10.1039/c5an02231b
16. **Li, C., Liu, W.J., Ren, Y.J., Sun, X.B., Pan, W., Wang, J.P.** The Selectivity of the Carboxylate Groups Terminated Carbon Dots Switched by Buffer Solutions for the Detection of Multi-metal Ions *Sensors and Actuators B* 240 2017: pp. 941 – 948. https://doi:10.1016/j.snb.2016.09.068
17. **Zhao, J.R., Pan, X.H., Sun, X.B., Pan, W., Yu, G.F., Wang, J.P.** Detection of Metronidazole in Honey and Metronidazole Tablets Using Carbon Dots-based Sensor via the Inner Filter Effect *Luminescence* 2018: pp. 1 – 9. https://doi:10.1002/bio.3467
18. **Jiang, K., Zhang, L., Lu, J.F., Xu. C.X., Cai, C.Z., Lin, H.W.** Triple-mode Emission of Carbon Dots: Applications for Advanced Anti-Counterfeiting *Angewandte Chemie International Edition* 55 2016: pp. 7231 – 7235. https://doi:10.1002/anie.201602445

© Dai et al. *2022* Open Access This article is distributed under the terms of the Creative Commons Attribution 4.0 International License (http://creativecommons.org/licenses/by/4.0/), which permits unrestricted use, distribution, and reproduction in any medium, provided you give appropriate credit to the original author(s) and the source, provide a link to the Creative Commons license, and indicate if changes were made.